Available online at www.sciencedirect.com

SciVerse ScienceDirect

Acta Materialia 61 (2013) 1266–1273

Acta MATERIALIA

www.elsevier.com/locate/actamat

Nonwetting "white graphene" films

Amir Pakdel *, Xuebin Wang, Yoshio Bando, Dmitri Golberg *

International Centre for Materials Nanoarchitectonics (MANA), National Institute for Materials Science (NIMS), Namiki 1-1, Tsukuba 305-0044, Japan

Received 18 August 2012; received in revised form 31 October 2012; accepted 1 November 2012
Available online 3 December 2012

Abstract

Nonwetting (superhydrophobicity) is currently of great interest in advanced materials research for self-cleaning applications, although it has been a well-known phenomenon in nature (e.g. in lotus leaves) for a long time. Aiming at widening the potential applications of synthetic superhydrophobic films, we have used a noncatalytic chemical vapor deposition method to prepare superhydrophobic films consisting of boron nitride (BN) nanosheets, also known as "white graphenes". A mixture of boron (B) and boron trioxide (B_2O_3) powder was used as a new precursor to grow such nano-rough films. The peculiar surface topography of the films induced a nonwetting behavior which was manifested by the picking up of external particles through water droplets rolling on their surface. The nonwetting tendency of the films is explained based on the interactions of the dipole moments of polar water molecules and BN nanosheets.

Keywords: Boron nitride nanosheets; Surface roughness; Dipole moments; Wetting; Self-cleaning

1. Introduction

Nanostructures consisting of a honeycomb network such as carbon nanotubes (CNTs) and graphenes have been in the forefront of materials science due to their unique properties and promising potential applications. A structural analogue of the carbon honeycomb lattice is hexagonal boron nitride (h-BN), in which C atoms are fully substituted with alternating B and N atoms. BN nanostructures exhibit diverse one-dimensional (1-D) and two-dimensional (2-D) morphologies, such as BN nanotubes (BNNTs), nanoribbons (BNNRs) and nanosheets (BNNSs) [1–3]. A hexagonal BN sheet and graphene have nearly identical lattice parameters, but, unlike graphene, BNNSs do not absorb light in the visible region of the electromagnetic spectrum and thus are called "white graphenes". In contrast to the semimetallic nature of graphite, BN is a semiconductor with a wide band gap of ~6 eV and possesses much higher chemical and thermal stability than its graphitic counterpart [4]. To date, extensive research has been conducted on the synthesis of BNNTs and their properties, suggesting many propitious applications such as gas absorbers, polymeric composites, electrical nanoinsulators, electron field emitters, ultraviolet photodetectors and hydrogen accumulators [4–9]. It is thus expected that other BN nanostructures, such as BNNSs, may also demonstrate interesting properties and find innovative utilizations in various areas.

Highly hydrophobic coatings and films are currently of increasing research interest and a number of methods have been established to produce such nonwetting surfaces [10]. In general, wettability of a surface depends on its chemical composition and microstructural geometry. Nonwetting surfaces with large water contact angles (CAs) can be prepared via two approaches: (1) chemical functionalization of the surface with materials of low surface free energy; (2) creating micro/nanoscale roughness on the surface [11]. Superhydrophobic surfaces exhibit extreme water-repellency, i.e. water droplets resting on them exhibit contact angles larger than 150°. Although water can easily wet the bulk BN surface (i.e. BN surface shows hydrophilicity), the films consisting of BN nanostructures have

* Corresponding authors. Tel.: +81 29 860 4696; fax: +81 29 851 6280.
E-mail addresses: PAKDEL.Amir@nims.go.jp (A. Pakdel), GOLBERG.Dmitri@nims.go.jp (D. Golberg).

1359-6454/$36.00
http://dx.doi.org/10.1016/j.actamat.2012.11.002

demonstrated ultrahydrophobicity [12–15]. There have been many reports on superhydrophobic films made of organic materials with low surface free energies, such as silicon-based hydrocarbons [16] and fluorinated polymers [17]. Also, several works on surface roughening have been performed, such as making electrodeposited gold cluster films [18], anodic oxidation of aluminum [19], fabricating aligned CNTs [20], producing films of zinc oxide (ZnO) [21] and synthesizing titanium oxide (TiO_2) nanowires [22]. However, unlike BN, most of these materials are not applicable at either high temperatures or harsh environments (e.g. highly acidic or alkaline media).

Recently we have reported the synthesis of BNNS films on silicon/silicon dioxide (Si/SiO_2) substrates by thermal chemical vapor deposition (CVD) of B, magnesium oxide (MgO) and iron oxide (FeO) powder under ammonia (NH_3) gas flow [13]. To investigate the effect of the initial precursor materials on the growth and properties of such films and to increase the activity of the precursors, in this work MgO and FeO were replaced by another oxidant, B_2O_3. The obtained BN films had nano-rough surfaces and exhibited superhydrophobicity and self-cleaning ability. To find clues about the roots of their nonwetting behavior, a density functional theory (DFT) method was utilized. Such water-repelling films are envisaged to find smart applications in surface protection of portable electronic products, non-fogging displays, medical and optical devices and anticorrosive equipments.

2. Experimental details

The crystalline BN nanosheets were grown via a CVD method in a horizontal tubular electric furnace. Elemental B and B_2O_3 powders were mechanically mixed and positioned in an alumina combustion boat covered with a Si/SiO_2 substrate. The boat was then set into a quartz test tube inside a vacuum chamber. The chamber was evacuated to ~1 torr and then ammonia gas was introduced at the rate of 0.4 ml min^{-1}. The precursors were heated to 1200 °C, held for 60 min and then cooled to room temperature.

The morphology and chemical composition of the films were studied by a field emission scanning electron microscope (FE-SEM; Hitachi S4800) equipped with an energy dispersive X-ray spectrometer (EDX). Structural features of the nanosheets were investigated by a high-resolution field-emission transmission electron microscope (HRTEM; JEOL JEM-2100F) equipped with an electron energy loss spectroscopy (EELS) detector. The topographical images of the films were obtained by a JEOL JSPM-5200 scanning probe microscope in the tapping atomic force microscopy (AFM) mode at ambient conditions. The water contact angle (CA) measurements were carried out by a sessile drop method using deionized water droplets of ~8 to 16 μl volume positioned on the films using a microsyringe. A high resolution Keyence VH-5000 optical instrument equipped with WinROOF V5.03 analysis software was used for measuring the water CA.

To compare the dipole moments of perfect and wrinkled BN surfaces, electronic structure calculations were performed within the context of density functional theory (DFT), using the Perdew–Burke–Ernzerhof [23], exchange–correlation functional and projected augmented wave methods, as implemented in the VASP code [24]. In all calculations, the corresponding Brillouin zone was sampled by a $4 \times 4 \times 1$ Monkhorst–Pack mesh [25].

3. Results and discussion

Fig. 1a and b displays SEM images of a typical film covering a large area. The nanosheets are uniformly distributed, well-separated and tend to be vertically aligned. The compact morphology of the present BNNSs is similar to that of nanosheets previously prepared by us [13], where a mixture of B, FeO and MgO powders was used as the initial precursor. Although the aforementioned mixture has been found to be an effective source for the growth of BN nanostructures, the formation of $Mg_2B_2O_5$ during the synthesis can reduce the chemical activity of the precursor and consequently hinder the growth of BN nanomaterials [26]. Thus, it is worth finding substitute compounds for precursor materials. Fig. 1a and b indicates that B_2O_3 could be considered as an alternative to MgO and FeO. This suggests that the growth of BNNSs is not strongly dependent on specific precursor materials, as long as enough reactive B and N atoms are provided in the growth atmosphere. Fig. 1c illustrates our suggested model for the two-stage growth of the present BNNSs. After nucleation and primary growth of preferential crystal planes with high growth rate on the substrate, a BN layer could form. Then, at the boundaries between neighboring sheets, top atomic layers could curl up due to the existence of force between them and vertical growth initiated. At last, these thin walls of BNNSs grew taller and formed the peculiar nano-rough morphology of the film.

The BNNSs were characterized by TEM as shown in Fig. 2a and b. The low magnification TEM image in Fig. 2a displays bent and scrolled nanosheets, as was anticipated as an intrinsic feature in 2-D nanostructures. The dark sections in Fig. 2b are the cross-sections of the BNNSs folded back and imaged edge-on. The observed transparency of the nanosheets to the electron beam indicates that they are atomically thin. The HRTEM image in Fig. 2b shows highly ordered lattice fringes, indicating that the BNNSs are well-crystallized. The average distance between adjacent fringes is ~0.33 nm, signifying that the regarded lattice fringes correspond to (002) crystal planes of h-BN. Curled edges of nanosheets made it possible to evaluate the sheet thicknesses from the HRTEM images. Having checked several sections in different HRTEM images, it was concluded that the majority of the BNNSs were less than 5 nm in thickness.

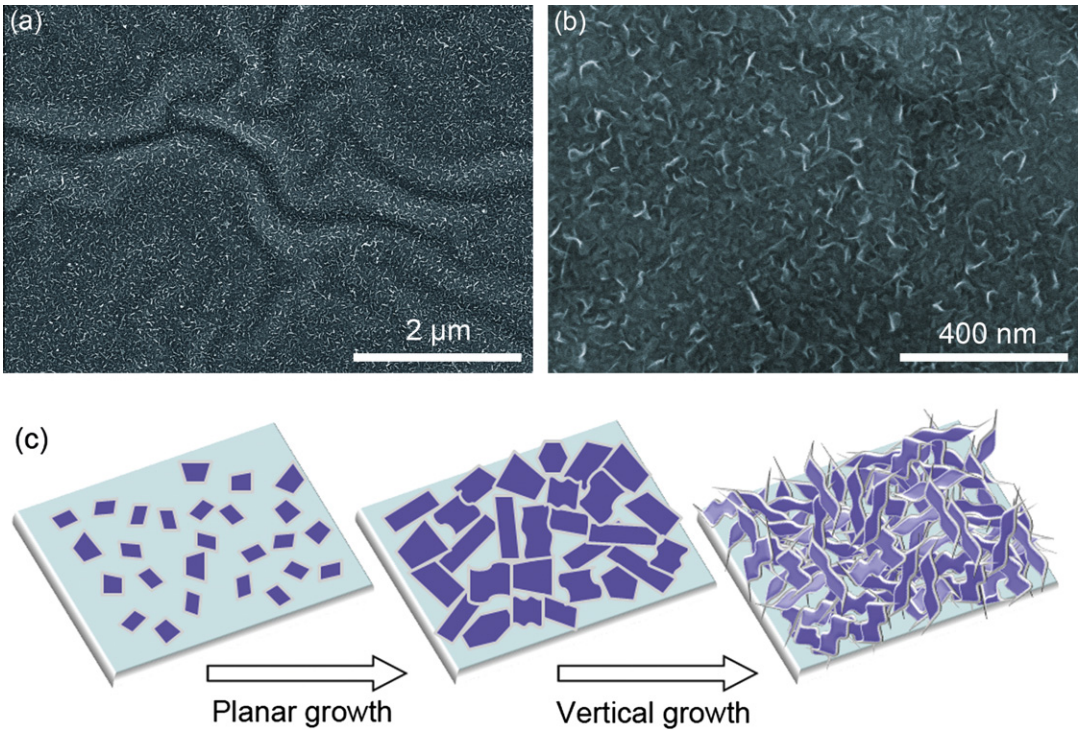

Fig. 1. (a, b) Typical SEM images of BNNSs indicating their uniform distribution on the substrates. (c) A model illustrating nucleation and two-stage growth of BNNSs on the substrate.

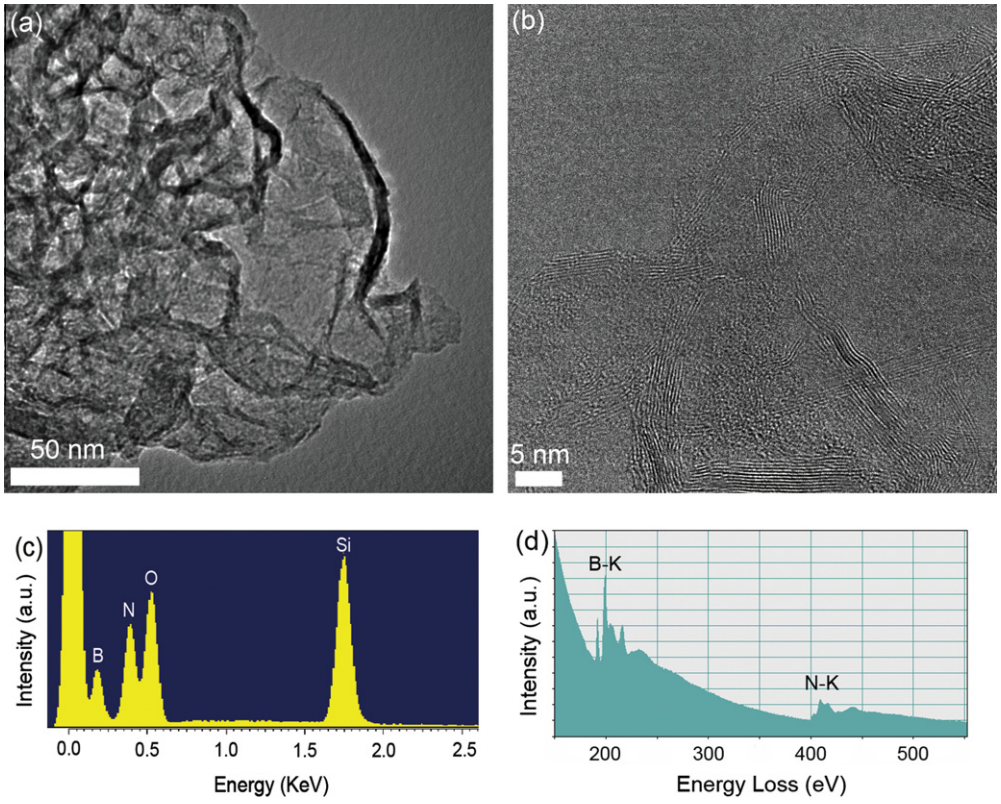

Fig. 2. (a) Typical TEM and (b) HRTEM images of BNNSs; and their (c) EDX and (d) EEL spectra.

The chemical composition and stoichiometry of the BNNSs were examined by EDX and EELS. Fig. 2c shows typical results of the EDX analysis over a large area of the product, indicating that the BNNSs are only composed of

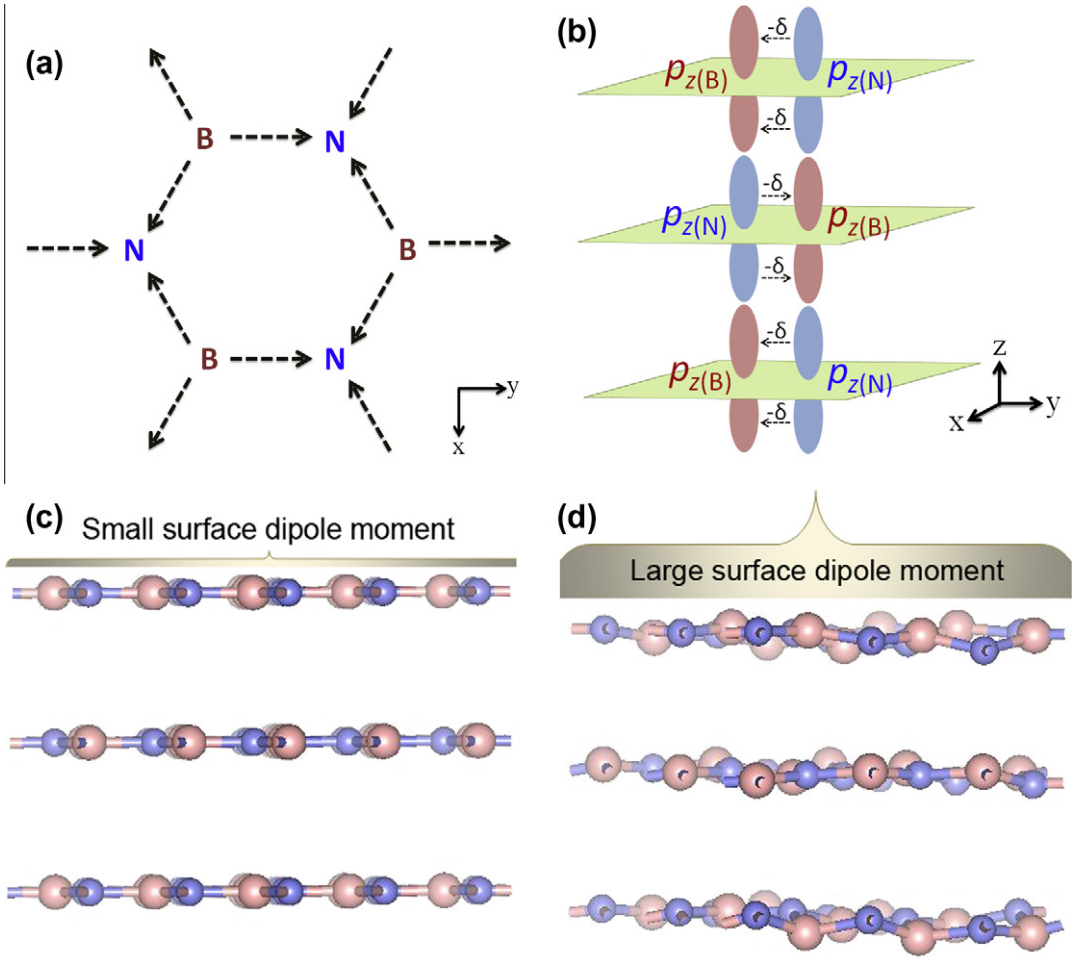

Fig. 3. (a) Charge transfer along the sp^2–σ bonds in BN. (b) Limited sharing of nitrogen pz(N) electron pair with boron pz(B) (partially available for π-bonding). (c) Atomically flat and (d) wrinkled BN sheets used in DFT simulations to compare their surface dipole moments.

B and N species covering the Si/SiO_2 substrate. Fig. 2d displays a typical EEL spectrum of the BNNSs having two distinct absorption features at 188 and 401 eV related to B and N K-shell ionization edges, respectively. The sharp peaks on the left and the right sides of the B–K and N–K edges correspond to 1s–π^* and 1s–σ^* antibonding orbits, respectively. This type of EELS edge structure is typical of sp^2-hybrizied layered BN materials. No trace of impurities was observed in the EEL spectrum, and quantification analysis gave a stoichiometric B:N atomic ratio of ~1:1.

The wettability of atomically flat and homogeneous surfaces, such as graphenes and BN sheets, is mainly determined by the chemical properties of their surfaces [27]. Some experimental studies have demonstrated that BN thin films exhibit higher wettability (hydrophilicity) than the graphene sheets, as they yield smaller contact angles of 51–67° [12,13]. The higher hydrophilicity of the BN films can be attributed to the polar nature of B–N bonds, which can enhance their interaction with polar water molecules. However, recent quantum molecular dynamics (QMD) simulations indicate that the diffusivity of water and the contact angle of water nanodroplets on atomically flat graphene and BN sheets are very similar. The simulated contact angle on a flat monolayer BN sheet is 86°, which is much larger than the reported experimental values. But simulation of a water droplet on a wrinkled monolayer BN sheet results in a notably smaller contact angle, due to the appearance of vertical dipoles on the wrinkled surface [28]. Since it is extremely difficult to achieve a perfectly flat BN sheet without wrinkles and defects in the experiment, local dipoles normal to the BN sheet appear, which could render the experimentally measured contact angle of water droplets considerably smaller than the computed ones.

Based on molecular orbital theory, three hybridized sp^2 orbitals exist for both B and N due to combination of one 2*s*-orbital with two 2*p*-orbitals ($2p_x$ and $2p_y$). These planar σ bonds are formed around each atom. Due to the difference in electronegativity of B and N, certain charge transfer along the sp^2–σ bonds takes place, which results in polar BN bonds, as illustrated in Fig. 3a. However, owing to the hexagonal structure symmetry, the overall dipole moment of the surface in *x* and *y* directions is zero. On the other hand, a non-hybridized p_z atomic orbital remains on each component, which is perpendicular to the plane of

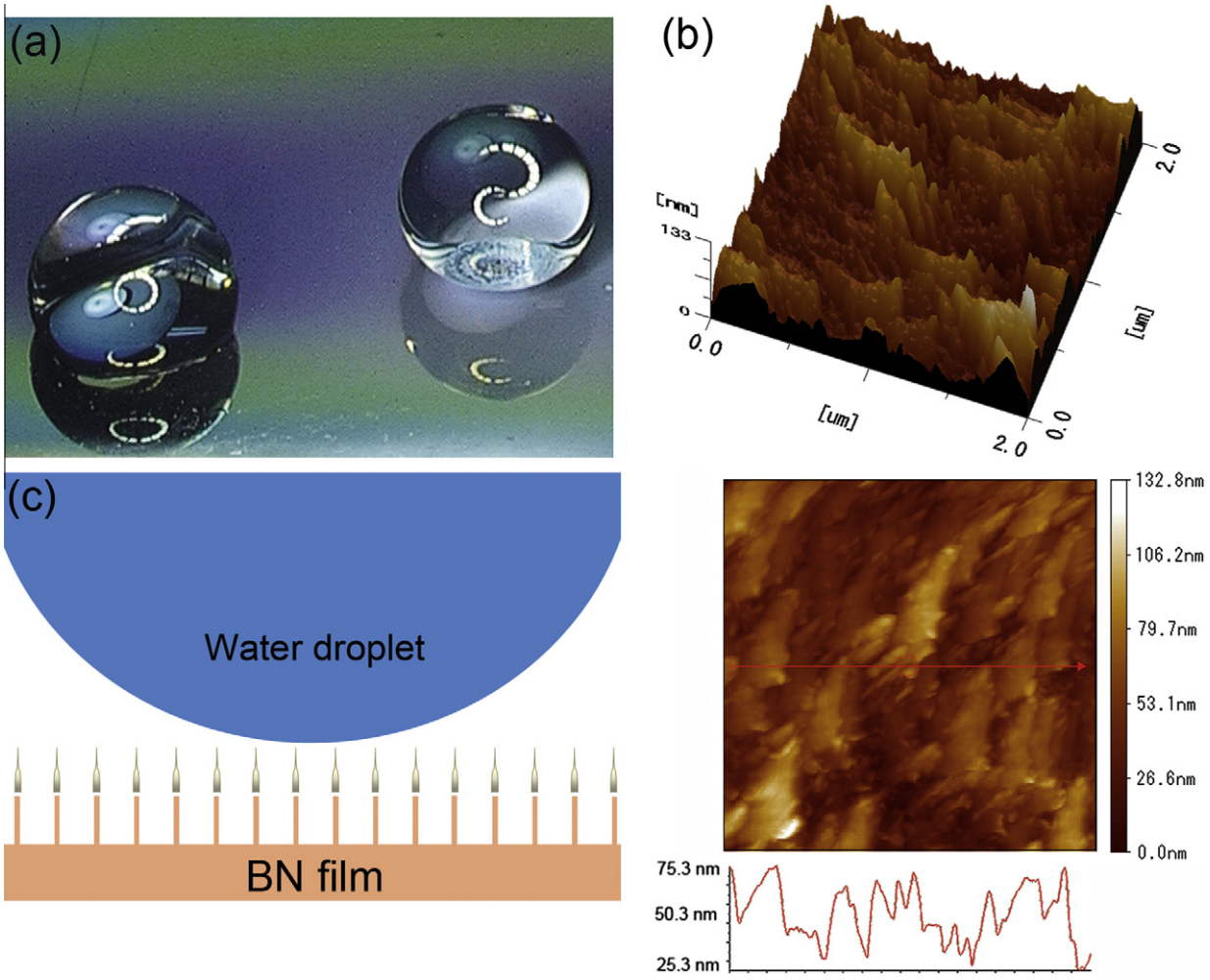

Fig. 4. Round water droplets on a BNNS film indicating its superhydrophobic behavior. (b) Representative AFM images of a BNNS film. (c) Schematic illustration of the limited surface interaction of a BNNS film and a water droplet.

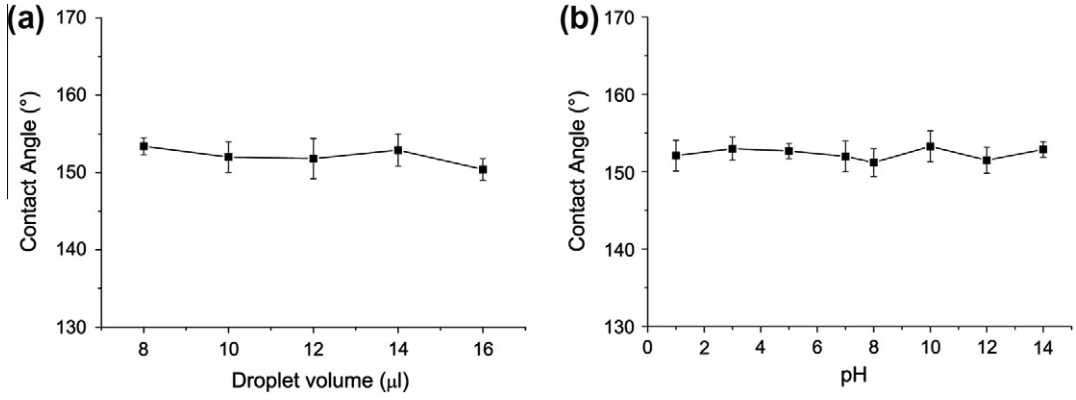

Fig. 5. Effect of (a) a water droplet size and (b) pH variations on water contact angle.

the three sp^2 orbitals. Two electrons with opposite spins in N are assumed to occupy $p_{z(N)}$, but in B, $p_{z(B)}$ remains empty. Thus, the two $p_{z(N)}$ electrons might be in part available for π-bonding, via the partial transfer of electrons from $p_{z(N)}$ to $p_{z(B)}$. This does not compensate the charge transfer along the sp^2–σ bonds from B to N, but can cause finite interactions of p_z orbitals in succeeding atomic sheets in multilayer BN, as shown in Fig. 3b. Since the upper p_z orbitals in the foremost layer do not interact with any other p_z orbitals, limited dipole moments can exist in z direction, normal to the atomic plane of BN. This was confirmed by our DFT simulations, where three BN layers consisting of

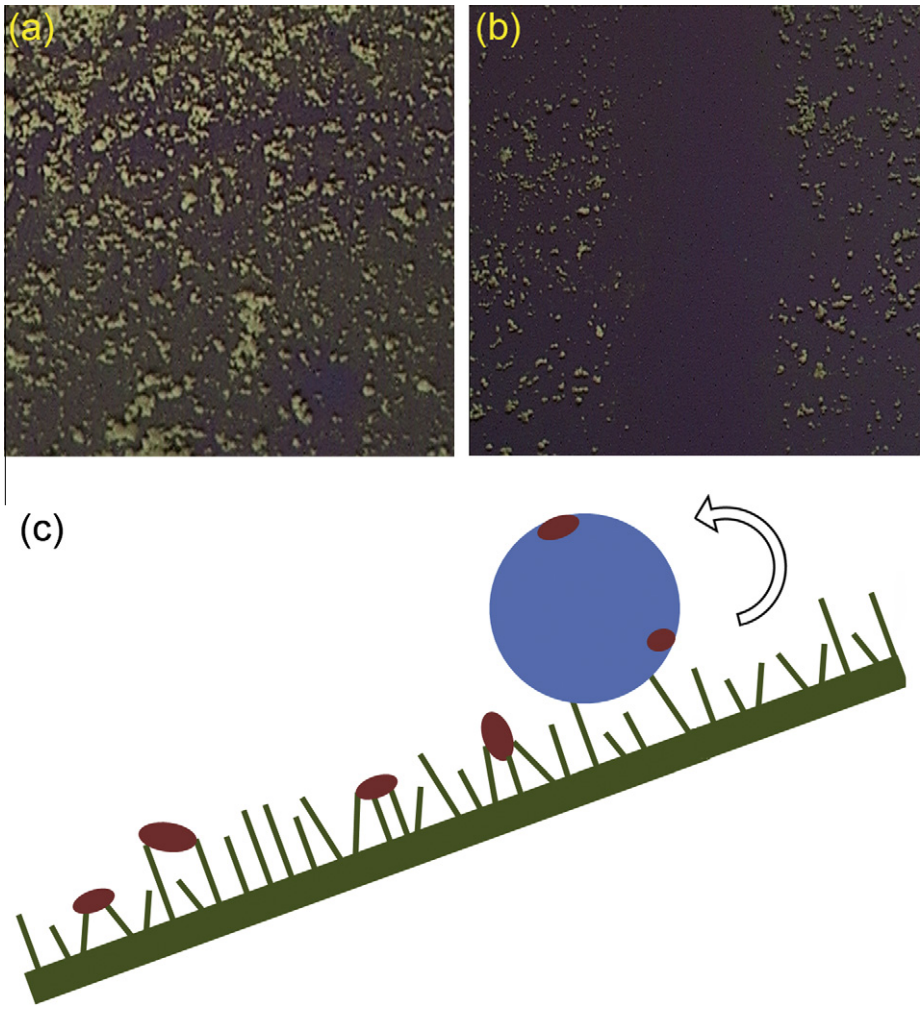

Fig. 6. (a) An optical microscope image showing randomly distributed MgO microparticles on a BNNS film. (b) Self-cleaning feature of the film after passing water droplets. (c) Illustration of the self-cleaning process under water droplet rolling off the surface.

27 B and 27 N in the periodic super cell ($3 \times 3 \times 1$ BN unit cell) were utilized, as schematically depicted in Fig. 3c. The calculated dipole moment in this condition was $\sim 10^{-3}$ Debye per unit cell. However, when we simulated wrinkles with random displacement of B and N atoms of the perfect BN layer in the z direction (between -0.5 and 0.5 Å), the dipole moments on the surface significantly increased to $\sim 10^{-1}$ Debye per unit cell. This can be attributed to the contribution of the B–N bonds that are not parallel to the xy plane in the wrinkled structure. In fact, the σ-related dipole moment components in the z direction could intensify the overall dipole moment on the surface, as schematically illustrated in Fig. 3d. Theoretical studies show that an increase in the dipole moment of a surface can largely intensify its wettability [27].

Fig. 4a displays the round shape of deionized water droplets with ~10 μl volume on the present film. The measured contact angle was ~152°, which indicates the superhydrophobic behavior of the pure BNNS film without applying any additional coating. A typical AFM image of a BNNS film and its corresponding height profile are shown in Fig. 4b. Quantitative AFM measurements showed that the maximum height difference on the film surface and its root mean square (rms) roughness were ~133 and ~20 nm, respectively. Such peculiar morphology with nanoscale roughness can generate hydrophobic behavior in contact with water droplets [29]. The classical principles of superhydrophobicity have been outlined in two models by Wenzel [30] and Cassie–Baxter [31]. The Wenzel model suggests that if liquid contact follows the contours of a rough surface, the effect of roughness should be to emphasize the intrinsic wetting tendency towards either film formation or enhanced contact angle. However, the Cassie–Baxter model indicates that when it is energetically favorable for a liquid to bridge across the tops of surface features, the droplet rests on a composite surface consisting of flat solid tops and air pockets between them [10]. Usually the surfaces that follow the Wenzel model show a sticky behavior toward water droplets (i.e. drops of water tend to adhere to them more than to a flat surface of the same type), but those that follow the Cassie–Baxter model show a slippery behavior (i.e. drops of water can roll off

more easily compared to an equivalent flat surface). In the case of the present BNNS films, when they were tilted, the water droplets easily rolled off the surface. It suggests that the surface follows the Cassie–Baxter model. Based on the SEM and AFM images of the present BNNS films, a schematic illustration of their surface is shown in Fig. 4c. If we consider the composite (BN/air) structure interfacing with a water droplet, the fraction of BN in contact with liquid is very limited. As a result, the overall interaction of BN dipole moments and water molecules is small. Therefore, the interaction of water molecules with themselves and the surrounding atmosphere (air) becomes crucial in determining the final shape of the droplet on the surface. The surface tension of the water droplet gives it a near-spherical shape, because a sphere has the smallest possible surface-area-to-volume ratio. Considering the limited interaction of the droplet with the present BNNS films, the droplet keeps its near-spherical shape, giving superhydrophobic features to the surface.

The effect of water-droplet size on contact angle is illustrated in Fig. 5a. The size of the droplets was altered from ~8 to ~16 μl, but this did not have any significant influence on the measured contact angles. The early literature on the effect of droplet size on contact angle measurements suggested the important role of the gravitational force [32]. However, this hypothesis was later rejected [33], and further experiments with liquids of varying density on several systems also confirmed the negligible contribution of the gravitational force to the size-related contact angle measurements. The present results indicate the stable water-repelling behavior of the BNNS films. Moreover, the BNNS films demonstrated stable nonwetting properties over a wide range of the liquid pH, as depicted in Fig. 5b. It indicates that even strongly acidic and alkaline conditions did not influence the superhydrophobic performance of the BNNS films due to their outstanding chemical inertness.

Motivated by the self-cleaning properties of naturally rough surfaces, such as lotus leaves, self-cleaning efficiency of the present nano-roughened BN films was investigated. In nature, water droplets roll off the superhydrophobic lotus leaves at a small sliding angle due to their rough surfaces made of papillose epidermal cells and an additional layer of epicuticular waxes. This special morphology of the leaves helps the liquid droplets to pick up contaminating particles and carry them away while rolling off the leaves. As shown in Fig. 6a, MgO microparticles were randomly pre-distributed on a BNNS film. Then the surface was tilted by 20° and a syringe was used to release a droplet of water from a very close distance to the surface. Fig. 6b demonstrates nearly complete cleaning along the droplet rolling-off path. If the adhesion between the particle and the coating surface (originating from the van der Waals forces) is overcome by the particle–water adhesion, the particles can be washed away by the droplet without redepositing in the path [34], as depicted in Fig. 6c. The adhesion between the particle and the BNNS film can be attributed to the micro/nano-roughness of the film, because on a rough surface the actual contact area between a particle and the surface is smaller than that of a smooth surface. Therefore, the smaller contact area would decrease the friction and adhesion of the particle to the surface, leading to a more efficient self-cleaning process.

4. Conclusions

Pure nano-rough h-BN films containing vertically aligned nanosheets were fabricated on Si/SiO_2 substrates via a noncatalytic CVD method, using B and B_2O_3 powder as precursor materials. The purity of the synthesized films was confirmed by X-ray energy dispersive and electron energy loss spectroscopy. It was suggested that the growth of such BNNS films may not be strongly dependent on specific precursor materials, as long as enough reactive B and N atoms are provided by the precursors in the growth atmosphere. The peculiar surface roughness of the films provided them with an excellent nonwetting behavior and stable self-cleaning ability. The superhydrophobicity of the films was discussed based on the interaction of dipole moments in BN sheets and water molecules.

Acknowledgments

This work was supported by the World Premier International (WPI) Center for Materials Nanoarchitectonics (MANA) of the National Institute for Materials Science (NIMS), Tsukuba, Japan. A.P. is grateful to Prof. Tomonobu Nakayama and Dr. Mohammad Khazaei for fruitful discussions, and MANA staff for their technical support. D.G. also acknowledges a "Mega-Grant" award for leading scientists tenable at the National University of Science and Technology "MISIS", Moscow, Russian Federation, under the Agreement No. 11.G34.31.0061.

References

[1] Golberg D, Bando Y, Huang Y, Terao T, Mitome M, Tang CC, et al. ACS Nano 2010;4:2979.
[2] Golberg D, Bando Y, Tang CC, Zhi CY. Adv Mater 2007;19:2413.
[3] Pakdel A, Zhi C, Bando Y, Golberg D. Mater Today 2012;15:256.
[4] Yu J, Qin L, Hao YF, Kuang S, Bai XD, Chong YM, et al. ACS Nano 2010;4:414.
[5] Chen ZG, Zou J, Liu QF, Sun CH, Liu G, Yao XD, et al. ACS Nano 2008;2:1523.
[6] Wang JS, Kayastha VK, Yap YK, Fan ZY, Lu JG, Pan ZW, et al. Nano Lett 2005;5:2528.
[7] Ma RZ, Bando Y, Zhu HW, Sato T, Xu CL, Wu DH. J Am Chem Soc 2002;124:7672.
[8] Zhi CY, Bando Y, Tang CC, Honda S, Sato K, Kuwahara H, et al. Angew Chem Int Ed 2005;44:7929.
[9] Khazaei M, Bahramy MS, Venkataramanan NS, Mizuseki H, Kawazoe Y. J Appl Phys 2009:106.
[10] Roach P, Shirtcliffe NJ, Newton MI. Soft Matter 2008;4:224.
[11] Feng L, Li SH, Li YS, Li HJ, Zhang LJ, Zhai J. Adv Mater 2002;14:1857.
[12] Li GX, Liu Y, Wang B, Song XM, Li E, Yan H. Appl Surf Sci 2008;254:5299.

[13] Pakdel A, Zhi CY, Bando Y, Nakayama T, Golberg D. ACS Nano 2011;5:6507.
[14] Li LH, Chen Y. Langmuir 2010;26:5135.
[15] Lee CH, Drelich J, Yap YK. Langmuir 2009;25:4853.
[16] Han JT, Xu XR, Cho KW. Langmuir 2005;21:6662.
[17] Morra M, Occhiello E, Garbassi F. Langmuir 1989;5:872.
[18] Zhang X, Shi F, Yu X, Liu H, Fu Y, Wang ZQ. J Am Chem Soc 2004;126:3064.
[19] Tsujii K, Yamamoto T, Onda T, Shibuichi S. Angew Chem Int Ed 1997;36:1011.
[20] Gomathi A, Harika MR, Rao CNR. Mater Sci Eng A – Struct 2008;476:29.
[21] Feng XJ, Feng L, Jin MH, Zhai J, Jiang L, Zhu DB. J Am Chem Soc 2004;126:62.
[22] Lai YK, Lin CJ, Wang H, Huang JY, Zhuang HF, Sun L. Electrochem Commun 2008;10:387.
[23] Perdew JP, Burke K, Ernzerhof M. Phys Rev Lett 1997;78:1396.
[24] Kresse G, Furthmuller J. Comp Mater Sci 1996;6:15.
[25] Monkhorst HJ, Pack JD. Phys Rev B 1976;13:5188.
[26] Zhi CY, Bando Y, Tan CC, Golberg D. Solid State Commun 2005;135:67.
[27] Giovambattista N, Debenedetti PG, Rossky PJ. J Phys Chem B 2007;111:9581.
[28] Li H, Zeng XC. ACS Nano 2012;6:2401.
[29] Shirtcliffe NJ, McHale G, Atherton S, Newton MI. Adv Colloid Interface Sci 2010;161:124.
[30] Wenzel RN. Ind Eng Chem 1936;28:988.
[31] Cassie ABD, Baxter S. Trans Faraday Soc 1944;40:546.
[32] Mack GL. J Phys Chem 1935;40:159.
[33] Collins RE, Cooke CE. Trans Faraday Soc 1959;55.
[34] Barthlott W, Neinhuis C. Planta 1997;202:1.